Nanocomposites Formed by Ion Implantation: Recent Developments and Future Opportunities

A. Meldrum[*1], L.A. Boatner[2], C.W. White[2]

[1]Department of Physics, University of Alberta, Edmonton, AB T6G 2J1 Canada
[2]Solid State Division, Oak Ridge National Laboratory, Oak Ridge, TN 37831 USA

Abstract

Ion implantation is a versatile and powerful technique for forming many types of nanocrystalline precipitates embedded in the near-surface region of a wide variety of crystalline and amorphous host materials. The unique optical, electronic, and magnetic properties of these nanocomposites has stimulated considerable recent research interest. In this review, we discuss recent developments in the field as well as some of the problems that currently hinder the potential applications of nanocomposites formed by ion implantation.

Keywords: ion implantation, nanocrystals, optical properties, magnetic properties

1. Introduction

In recent years, an increasing level of research interest has concentrated on the unique structure and properties of many types of nanocrystalline materials. Owing to their size-dependent electronic properties, materials composed of discrete, isolated nanocrystals (NCs) have a wide range of potential applications. Many techniques have been developed for the synthesis of nanocrystals, each with specific advantages and disadvantages. Ion implantation is a method that is becoming increasingly important in this field, and a considerable body of literature now exists on the formation and properties of NCs formed by ion implantation techniques. In this method, energetic ions are injected into the near surface region of a selected host material. During implantation or in a subsequent thermal processing step, the implanted material nucleates as discrete precipitates located in a thin (< 1 μm) layer near the surface of the host.

The increasing popularity of the ion implantation technique is partly due to the fact that the overall near-surface nanocomposite structure has characteristics that represent important technical advantages over conventional thin films or homogeneous bulk nanophase materials. For example, useful properties of two or more precipitated phases can be combined into one well-defined, integrated structure, and the important physical properties of the nanocomposite can be optimized for a particular application by controlling the concentration and size of the precipitates. Ion implantation can be readily combined with many other experimental techniques for the creation of novel materials. Additionally, nanocomposites formed by ion implantation are durable - the NCs are protected from the surrounding environment because they are formed below the surface and become an integral part of the host material. Despite these advantages, several problems currently restrict the use of this type of nanocomposite in actual devices. One long-standing problem has been the relatively wide particle size distributions. Recent efforts to address this issue have met with moderate success [1], and additional experiments are underway to further elucidate methods of size control. Another problem is the effect of radiation-induced defects and structural modifications that occur in the host during implantation. Radiation effects can complicate the microstructure and the optical properties of the resulting nanocomposite. In addition, the nature of the interface between the precipitates and the host is generally not well understood, leading to some uncertainty in determining the origin of certain optical effects.

The following review highlights recent work on metallic precipitates for nonlinear optics and on semiconductor NCs for

* Corresponding author: tel: 1-780-492-5342; fax 1-780-492-0714; e-mail: ameldrum@ualberta.ca

controlled absorption, luminescence, and optical switching. In the final section, recent work on ferromagnetic NCs is discussed in light of their potential applications in magnetic recording. Outstanding problems and potential solutions are discussed.

2. Metallic Nanocrystals

Ion implantation has been used to produce metallic nanoclusters embedded in the near-surface region of a ceramic host, most commonly silica glass, for at least three decades [2]. It was recognized early on that ion implantation is a useful method for controlling the depth distribution of metallic NCs and that higher local concentrations of particles could be obtained than by conventional processing methods. Size and size distributions are, at least to some degree, controllable by varying the implanted-ion concentration. Optical properties of metallic nanoparticles embedded in a dielectric host are dominated by surface plasmon resonance (SPR) absorption, suggesting applications as optical filters [3], including eye-glass coatings [4]. Materials composed of a high volume density of metallic precipitates embedded in a dielectric also exhibit a large nonlinearity in the third-order optical susceptibility (χ^3) at the SPR frequency. Thus, the refractive index of the composite can be modified and controlled as a function of light intensity. These materials have potential applications in all-optical-memory or switching devices [e.g., Refs. 3,5,6], and ion implantation is a technique that appears ideally suited for the development of this type of nonlinear composite.

Owing in large part to the pronounced nonlinear effects and the associated applications, numerous types of metallic colloids have been formed by implantation into a variety of host materials. The optical absorption properties of gold NCs embedded in SiO_2 [7,8], Al_2O_3 [9-11], MgO [12 ,13], CaF_2 [14], and $KAl_2(Si_3Al)O_{10}(OH,F)_2$ (muscovite) [15] have been measured. In SiO_2, the precipitates are spherical and randomly oriented. SPR absorption is observed at approximately 530 nm, as predicted by Mie theory. For the smallest particle sizes, the plasmon band is relatively weak, slightly broadened, and is shifted to slightly higher energies due to quantum confinement. Similar effects have been observed for Ag NCs in SiO_2 [10,16 ,17], where the SPR bands are centered at 400-410 nm. Size distributions of Ag NCs tend to be bimodal with the larger precipitates occurring near the end of the implanted-ion range [16]. These larger NCs cause a widening the SPR absorption band and the formation of higher-order optical absorption bands at lower energy. Other metallic NCs formed by ion implantation of SiO_2 that show SPR absorption consistent with Mie theory include Sn, Cu, Zn, Fe, Mn, Ti, Ga, Cr, and Pb [18-24].

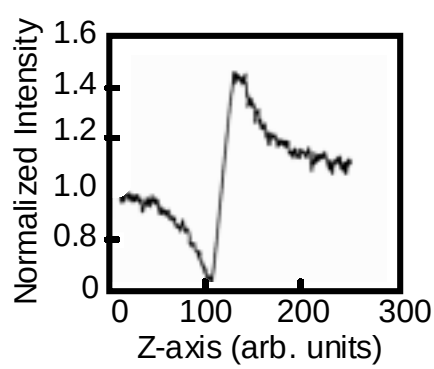

Fig. 1. Z-scan measurement for Au NCs in SiO_2. The change in intensity with Z-distance is consistant with a positive value of n_2. From the intensity results, n_2 was estimated to be 4.1 x 10^{-10} cm^2/W [7].

The nonlinear refractive index of metallic NCs (see Fig. 1) embedded in SiO_2 and Al_2O_3 is enhanced by 2-3 orders of magnitude over conventional quenched glasses [7,10,25], with picosecond response times. Unfortunately, linear and nonlinear effects are both maximized at the SPR frequency. This decreases the figure of merit for nonlinear optical devices [3] based on this technology, due to the high absorption and associated thermal effects. New methods are being developed to decrease the linear absorption coefficient while, at the same time, maintaining or enhancing the nonlinear susceptibility [26].

In one recent effort, metallic NCs of Au were formed in crystalline MgO. For gold NCs in MgO, the surface plasmon resonance frequency can be modified by defects in the host material. F_n centers (aggregates of *n* oxygen vacancies with 2*n* trapped electrons) are electron donors, thereby causing reversible shifts in the SPR energy from 560 to 520 nm [12]. Interaction of trapped electrons at defect centers with nearby metallic NCs provides an opportunity to tailor the SPR frequency and, potentially, to decrease the absorption coefficient. In another technique, multi-implantation protocols are being developed to modify the SPR frequency and enhance the nonlinear properties. One implanted element can be used as an impurity to increase the dielectric constant of the host, while the other is used to form precipitates. This

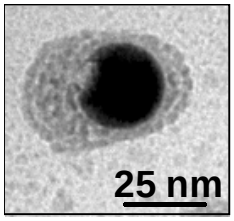

Fig. 2. Zn NC in SiO_2 glass. The particle is coated with a Zn-silicate reaction rim.

technique was demonstrated for Au NCs in Ti-implanted SiO_2, where the SPR wavelength was shifted from 530 to 560 nm due to the presence of Ti impurities in the host [27]. Alternatively, both implanted elements can be used to form particles. Ag-Sb and Ag-Cd intermetallic NCs have optical properties that are different from either pure constituent (essentially, the SPR of Ag grows weaker with increasing Sb [28]); whereas, Ag+Cd-implanted SiO_2 exhibits absorption that is consistent with a superposition of the SPR peaks from both Ag and Cd phases [29]. Similar types of effects have been observed for In-Ag, In-Cu, and Cu-Ni intermetallic nanocrystals [25,30]. There is new evidence for the formation of core-shell structures in twice-implanted specimens [31,32]. Zn nanocrystals with zinc-silicate "blankets" can be formed at high processing temperatures (Fig. 2). Core-shell structures are particularly interesting due to the change in the dielectric constant that occurs at the core-shell boundary. A model developed to calculate the optical density for coated NCs embedded in SiO_2 was recently applied to Cu-coated Ag NCs [32]. An additional benefit may be obtained in these specimens from the inverse cube dependence of the imaginary part of χ^3 on the diameter of the precipitates - below a composition-dependent fixed size limit - due to intraband electronic transitions [6]. In general, the recent efforts described above have as an objective the reduction in absorption of the specimen while maintaining good nonlinear properties.

These recent results demonstrate that the ion implantation technique can be used to form many types of novel precipitates (alloys or core-shell structures). Ion implantation provides a unique opportunity to tailor the properties of the nanocomposite – with the goal of improving the optical properties for future optical switching or all-optical-memory devices. Despite these recent advances, many questions remain concerning the microstructure and optical properties of embedded metallic nanoparticles. Means by which the size distributions may be better controlled are being actively explored using Monte Carlo simulations combined with transmission electron microscopy (TEM) measurements [33]. Percolation effects may also be important when particle densities are high. Techniques to decrease the absorption while maintaining high nonlinear susceptibility will increase the figure of merit for optical devices based on ion-implanted nanocomposites. The thermal contribution to the nonlinear susceptibility - which has a slow relaxation time - also remains problematic.

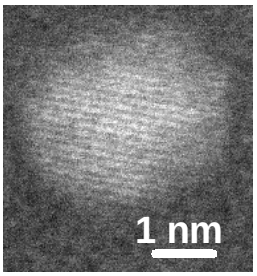

Fig. 3. Z-contrast image of a Si NC embedded in SiO_2.

3. Semiconductor Nanocrystals

Semiconductor nanocrystals formed by ion implantation of a dielectric produce composites that can also show strong nonlinearities in the third-order susceptibility with response times ranging from nanoseconds [34] to picoseconds [35]. The main interest in semiconductor NCs stems from the pronounced effects of quantum confinement and from the strong visible photoluminescence. Confinement of exciton wavefunctions increases the energy of the bandgap and divides it into a set of discrete levels [e.g., see Refs 3 and 36 for detailed theoretical descriptions of this effect]. The magnitude of these transitions depends on the electronic properties of the semiconductor, and it is enhanced for smaller particles sizes. Bandgap absorption is strongly dependent on particle size, and narrow size distributions are, therefore, necessary for observing the details of the size-dependent electronic transitions. The following discussion is limited to recent work on silicon, chalcogenide, and oxide semiconductor NCs – although considerable work has also been done on other phases (e.g., Ge, GaN, GaAs, and InP).

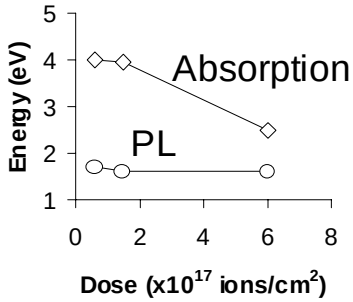

Fig. 4. Variation of PL and absorption energies with implant dose for Si NCs in SiO_2 [43].

Silicon NCs formed by ion implantation of SiO_2 emit a strong photoluminescence (PL) centered at 730-800 nm. Considerable controversy exists over the

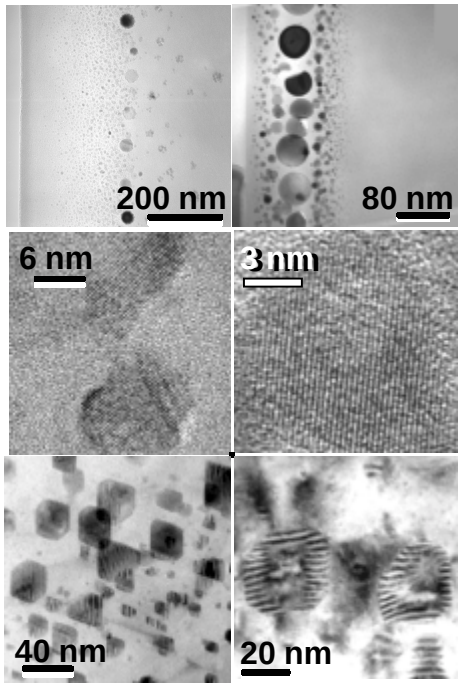

Fig. 5. Gallery of sulfide nanocrystals. Top left: ZnS NCs in SiO_2; Top right: PbS NCs in SiO_2; Middle left: Crystallographically oriented ZnS in amorphous silicon; Middle right: hollow CdS precipitate in SiO_2; Bottom left: faceted and aligned CdS NCs in Si; Bottom right: Hollow precipitates of $CdZnS_2$ in Si.

origin of the PL in Si-implanted SiO_2. The origin of this PL has been attributed to surface states [e.g., 37,38] and to recombination of confined excitons [e.g., 39-42]. We recently reported optical absorption and PL results from a suite of Si-implanted SiO_2 specimens [43]. The ion dose was varied to control the average NC size as measured by Z-contrast TEM analysis (Fig. 3). By using the annular dark-field detector, small differences in the average atomic number of the specimen can be readily observed as intensity variations, making this technique ideally suited for observing nm-sized Si particles in SiO_2. With decreasing implant concentration or dose, the average particle size decreased correspondingly from above 6 nm to less than 3 nm. Optical absorption spectra were obtained, and the absorption bandgap was extracted from the energy-absorption relationship for indirect gap semiconductors [44]. In Fig. 4, the PL energy and the absorption bandgap are plotted as a function of implant dose. Clearly, there is a large shift to higher energies in the absorption gap as the implant dose is decreased (and the particle size is correspondingly decreased); however, the PL energy remained nearly constant - centered at ~750 nm. These observations are evidence in favor of a quantum-confinement model for the optical absorption, but since the PL is relatively independent of particle size, the luminescence may be controlled by surface or interface states in these specimens. In one potential application, the size-graded absorption suggests that this type of composite has potential applications in advanced photovoltaic devices [45].

Large differences in PL intensity are obtained in different thermal processing atmospheres [39,46]. The presence of H or D in the processing atmosphere increases the luminescence by at least a factor of 4 [47]. Hydrogen depth profiles are consistent with monolayer coating on the surface of the nanoparticles [47]. These results support a model for increased radiative emission as a result of passivation of defects at the SiO_2-Si interface. Interestingly, Si precipitates formed in Al_2O_3 or MgO show virtually no luminescence, even when processed in a reducing atmosphere. Clearly, the SiO_2-Si interface has a unique property giving rise to strong PL that is not replicated at other Si-oxide interfaces.

We have also carried out extensive investigations of the properties of chalcogenide NCs (CdSe, CdS, ZnS, PbS) formed by ion implantation [48-52]. The microstructure of compound semiconductor NCs in SiO_2 is highly complex, and the size distributions tend to be wider than for single-element nanoparticles [48,53]. A gallery of unusual microstructures is presented in Fig. 5. From these images it can be seen that "conventional" implantation plus thermal processing conditions do not produce sufficiently narrow size distributions to observe sharp electronic transitions. Nevertheless, the precipitates show some interesting optical properties. There is convincing evidence for quantum confinement effects in CdS NCs [51]. The absorption bandgap shifts to higher energies with decreasing particle size, as measured by TEM (Fig. 6), and the magnitude of the shift is consistent with the theory for quantum confinement [54]. Relatively weak PL was observed at energies slightly

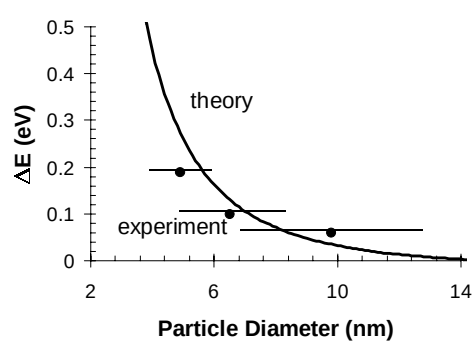

Figure 6. Bandgap shift (ΔE) vs. particle size for CdS NCs in SiO_2. Horizontal bars represent the size range of precipitates. Curved line is calculated from Ref. 54.

above the bandgap – also consistent with quantum confinement effects. CdS NCs in Al_2O_3 emit strong PL at energies that are also slightly above the bandgap of bulk CdS; however, this was attributed to strain effects since the particle sizes in Al_2O_3 were larger than the exciton radius [51]. The ZnS luminescence is weaker - although it may be enhanced by the subsequent implantation of Mn [55], and there is no clear evidence of quantum confinement.

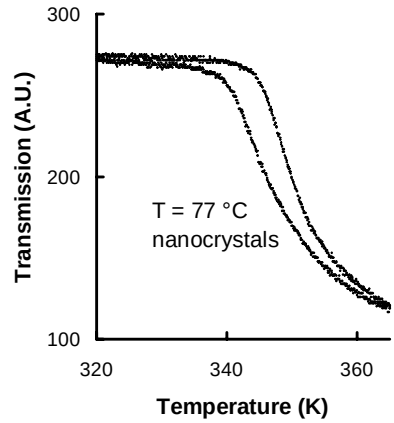

Fig. 7. Optical transmission as a function of temperature for VO_2 NCs in SiO_2 at a wavelength of 3.4 μm [59].

In order to enhance the PL from these chalcogenide NCs, it could be useful to form core-shell structures by ion implantation. The shell should passivate the interior surface and have a higher bandgap in order to maintain confinement in the core. Two-element Monte Carlo simulations suggest that the formation of core-shell structures by ion implantation should be possible, depending on the solubility of the respective elements and the amount of collisional mixing [56]. For compound semiconductor NCs such as ZnS-coated CdS, three elements are involved with up to four separate implantation steps. One simple option for creating core-shell structures might be to first form the core particles (e.g., CdS) by implantation of Cd+S followed by thermal processing, and subsequently implant material for the shell (e.g., Zn+S). During a final thermal processing step, the ZnS may coat the pre-existing CdS cores. In a preliminary experiment, we followed this procedure but formed a near 50-50 mixed chalcogenide composition $CdZnS_2$ instead of the desired core-shell structures, as determined by elemental mapping in the TEM [57]. Perhaps the thermal processing temperature (1000°C) was too high in this case. Another problem is that some of the second implant (Zn+S) is injected *into* pre-existing CdS cores. Further experiments are underway, but it is clear that forming uniform, highly luminescent compound sulfide core-shell structures will be a difficult challenge that will push the current limits of the implantation technique.

Semiconducting oxide NCs can also be formed by co-implantation techniques. Several transition metal oxides show large changes in their electronic structure across a crystallographic phase transition. VO_2 and V_2O_3 are particularly interesting in that the resistivity changes by several orders of magnitude at the phase transition temperature (~350 and ~150 K for VO_2 and V_2O_3, respectively). Accordingly, precipitates of VO_2 and V_2O_3 were formed by implantation of V+O into sapphire, followed by thermal processing [58,59]. Thermal processing conditions were used to control which phase was formed. A pronounced optical transition was observed at the metal-semiconductor transition temperature for both phases (e.g., Fig. 7), suggesting potential applications for this type of nanocomposite as durable optical sensors and switches.

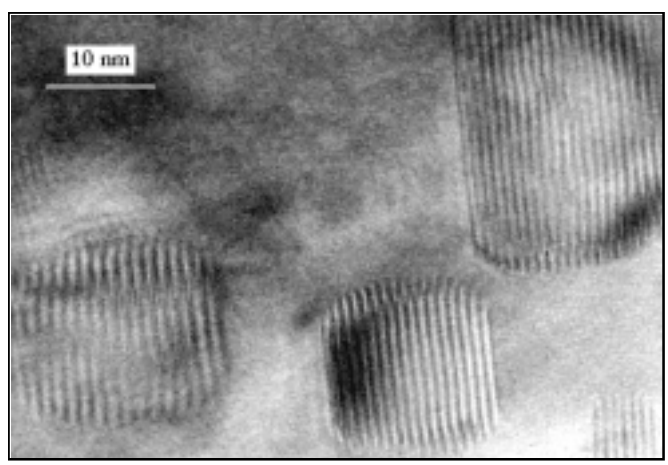

Fig. 8. Crystallographically oriented "nanocubes" of α-Fe embedded in YSZ.

4. Ferromagnetic Nanoparticles

Isolated ferromagnetic nanoparticles may represent the future of ultra-high-density magnetic data storage. Information density could be increased by up to 10,000 times over current devices if the ultimate goal of single-particle-per-bit data storage can be reached [60]. For single-particle bits to be written individually, the precipitates must be discrete, magnetically isolated, single domain ferromagnetic nanoparticles that are larger than the superparamagnetic limit and whose coercivity, size, orientation, and position can be controlled. Many techniques are being actively explored for the formation of this type of nanophase material [a

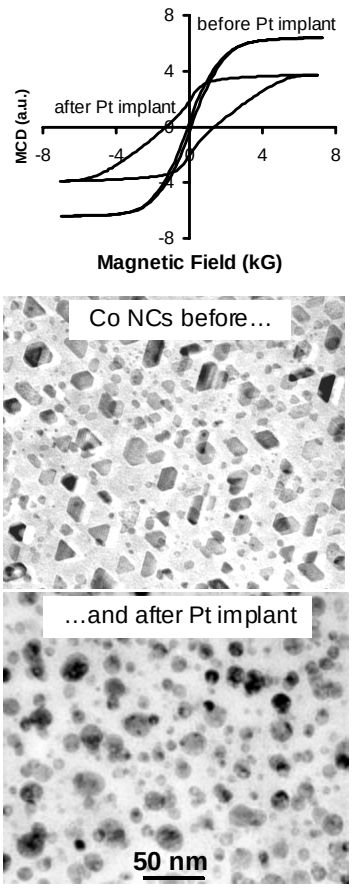

Fig. 9. Magnetic hysteresis results and corresponding microstructure for Co NCs in sapphire.

list of techniques is given in Ref. 61]. Ion implantation has been widely used for the processing of magnetic films. Recent efforts have conclusively demonstrated that the technique can, in fact, be used to form ferromagnetic nanoparticles that meet some of the requirements for ultra-high-density data storage [62-64].

Our recent investigations have focused on the properties of Fe and Ni nanoparticles formed by ion implantation of yttrium-stabilized (cubic) zirconia (YSZ) [65]. For the Fe-implantation of YSZ, either a ferromagnetic oxide (Fe_3O_4) or pure ferromagnetic metal (α-Fe) nanoparticles can be synthesized, depending on the thermal processing conditions. The NCs are well separated from each other by the host matrix so there are no grain boundaries and, therefore, no grain boundary effects. The particles are crystallographically aligned with one another and with the host, and they are generally well faceted (e.g., Fig. 8). Fe and Ni NCs show magnetic hysteresis with low coercivity (57 G and 50 G, respectively, for α-Fe and Ni at room temperature with the magnetization direction perpendicular to the specimen plane) [65]. At lower temperatures, the hysteresis loops are wider, consistent with the concept of blocking temperatures for smaller particles.

This preliminary work was recently extended to the case of Co NCs embedded in sapphire [66]. The precipitates were faceted along the {1000} set of planes in sapphire and are on-average ~15 nm parallel to their long axis (Fig. 9). At room temperature, the coercivity and remanence magnetization are 150 G and 4%, respectively. The coercivity of ferromagnetic Co thin films in commercial magnetic storage devices is increased by the addition of Pt [60]. Accordingly, the specimen described above was *subsequently* implanted with Pt to a fluence of approximately 10% of the original Co fluence. The resulting microstructure and magnetic hysteresis are shown in Fig. 9. That the NCs are still crystalline and aligned with the sapphire host was determined by electron diffraction (not shown), although minor streaking of the precipitate diffraction maxima suggested a small degree of misorientation. Nevertheless, the microstructure of the particles is radically different after the Pt implantation. The faceting has disappeared, and the NCs are spheroidal and show mottled contrast. The magnetic hysteresis curve is also different, with coercivity and remanence values increased to 1.14 kG and 46%, respectively. The shape of the hysteresis curve was strongly dependent on the orientation of the magnetic field: with the field parallel to the implanted surface, the coercivity of the Pt-implanted Co NCs was approximately 5 times smaller than with the field applied perpendicular. In order to distinguish between radiation damage and chemical effects, the Co-particle specimen shown in Fig. 9 (top micrograph) was implanted with Xe at a fluence chosen to give the same amount of displacement damage in the implanted region as for the Pt implant [66]. The increase in coercivity and remanence magnetization was only about half of that for Pt implanted sample, suggesting that both radiation damage and chemical effects are responsible for producing the high coercivity. These preliminary results demonstrate that the magnetic properties of ferromagnetic Co particles in a crystalline host can be controlled by subsequent ion implantation into the precipitate layer.

Clearly, ion implantation is a technique that could potentially find future applications in ultra-high density magnetic storage devices. Nevertheless, many important experimental difficulties remain. Microstructurally, co-implanted specimens must be characterized in detail. Temperature-dependent measurements will be required to better understand the magnetic properties. Investigations are underway using micromagnetics codes to simulate the ion implanted samples as a planar array of randomly spaced dipoles of mixed size, and to control the location and spacing of the precipitates.

Conclusions

Ion implantation is clearly a versatile and flexible tool for creating a large number of nanocrystal-host compositions with a wide range of optical, electronic, magnetic, and microstructural properties. In this brief review, some of the most promising properties and outstanding problems related to these nanocomposites were discussed. Many new advances will undoubtedly be made in the near future, including the use of focused-ion-beam techniques for producing ordered arrays; the use of ultra-fine-scale lithographic masks for controlling precipitate locations; and new processing techniques will be developed for the synthesis of more complex nanocomposites with novel electro-optic properties.

Acknowledgments
The principle author wishes to acknowledge the staff at the SMAC Facility, ORNL (Ray Zuhr, Ed Sonder, Dave Poker, Steve Withrow, Darrell Thomas, and Jim Williams) for their constant support and advice, both technical and scientific. Don Henderson of Fisk University has always been supportive and willing to discuss numerous scientific issues. Research was sponsored by the U.S. Department of Energy under contract DE-AC05-00OR22725 with the Oak Ridge National Laboratory, managed by UT-Battelle, LLC. AM is funded by an NSERC operating grant.

References
[1]A. Meldrum, E. Sonder, R.A. Zuhr, I.M. Anderson, J.D. Budai, C.W. White, L.A. Boatner, and D.O. Henderson, J. Mater. Res. 14 (1999) 4489.
[2]G.W. Arnold and J.A. Borders, J. Appl. Phys. 48 (1977) 1488.
[3]C. Flytzanis, F. Hache, M.C. Klein, D. Ricard, and Ph. Roussignol, Prog. Opt. 29, edited by E. Wolf (Amsterdam, North-Holland, 1991) p.321.
[4]M. Mennig, K. Endres, M. Schmitt, and H. Schmidt, J. Non-Cryst. Sol. 218 (1997) 373.
[5]P. Chakraborty, J. Mater. Sci. 33 (1998) 2235.
[6]L. Yang, D.H. Osborne, R.F. Haglund Jr., R.H. Magruder, C.W. White, R.A Zuhr, and H. Hosono, Appl. Phys. A 62 (1996) 403.
[7]C.W. White, D.S. Zhou, J.D. Budai, R.A. Zuhr, R.H. Magruder, and D.H. Osborne, Mat. Res. Soc. Symp. Proc. 316 (1994) 499.
[8]R.H. Magruder III, L. Yang, R.F. Haglund Jr., C.W. White, L. Yang, R. Dorsinville, and R.R. Alfano, Appl. Phys. Lett. 62 (1993) 1730.
[9]C.W. White, D.K. Thomas, R.A. Zuhr, J.C. McCallum, A. Pogany, R.F. Haglund, R.H. Magruder, and L. Yang, Mat. Res. Soc. Symp. Proc. 268 (1992) 331.
[10]C.W. White, D.K. Thomas, D.K. Hensley, R.A. Zuhr, J.C. McCallum, A. Pogany, R.F. Haglund, R.H. Magruder, and L. Yang, Nanostructured Materials 3 (1993) 447.
[11]D.O. Henderson, R. Mu, Y.S. Tung, M.A. George, A. Burger, S.H. Morgan, C.W. White, R.A. Zuhr, and R.H. Magruder, J. Vac. Sci. Technol. B 13 (1995) 1198.
[12]A. Ueda, Y.S. Tung, M. Wu, W.E. Collins, D.O. Henderson, C.W. White, R.A. Zuhr, J.D. Budai, A. Meldrum, P.W. Wang, and X. Li, Nucl. Instr. Meth. B141 (1998) 261.
[13]R.L. Zimmerman, D. Ila, E.K. Williams, S. Sarkisov, D.B. Poker, and D.K. Hensley, Nucl. Instr. Meth. B 141 (1998) 308.
[14]D.O. Henderson, Y.S. Tung, A. Ueda, R. Mu, Y. Xue, C. Hall, W.E. Collins, C.W. White, R.A. Zuhr, J.G. Zhu, and P.W. Wang, J. Vac. Sci. Technol. A 14 (1996) 1199.
[15]D.O. Henderson, R. Mu, A. Ueda, Y.S. Tung, C.W. White, R.A. Zuhr, and J.G. Zhu, J. Non-Cryst. Sol. 205-207 (1996) 788.
[16]M. Antonella, G.W. Arnold, G. Battaglin, R. Bertoncello, E. Cattaruzza, P. Colombo, G. Mattei, P. Mazzoldi, and F. Trivillin, J. Mater. Chem. 8 (1998) 457.
[17]Z. Liu, H. Li, X. Feng, S. Ren, H. Wang, Z. Liu, and B. Lu, J. Appl. Phys. 84 (1998) 1913.
[18]E. Johnson, A. Johansen, L. Sarholdt, and U Dahmen, Nucl. Instr. Meth. B 148 (1999) 1034.
[19]L.C. Nistor, J. Van Landuyt, J.D. Barton, D.E. Hole, N.D. Skelland, and P.D. Townsend, J. Non-Cryst. Sol. 180 (1995) 266.
[20]J. Stark, R.A. Weeks, D.L. Kinser, and R.A. Zuhr, J. Non-Cryst. Sol. 95&96 (1987) 685.

[21]R.H. Magruder III, D.O. Henderson, S.H. Morgan, and R.A. Zuhr, J. Non-Cryst. Sol. 152 (1993) 258.
[22]Y. Takeda, T. Hioki, T. Mohohiro, S. Noda, and T. Kurauchi,, Nucl. Instr. Meth. B 91 (1994) 515.
[23]G. Whichard, H. Hosono, R.A. Weeks, R.A. Zuhr, and R.H. Magruder III, J. Appl. Phys. 67 (1990) 7526.
[24]Z. Pan, S.H. Morgan, D.O. Henderson, S. Park, R.A. Weeks, R.H. Magruder III, and R.A. Zuhr, Mat. Res. Soc. Symp. Proc 316 (1994) 469.
[25]M. Falconieri, G. Salvetti, E. Cattaruzza, F. Gonella, G. Mattei, P. Mazzoldi, M. Piovesan, G. Battaglin, and R. Polloni, Appl. Phys. Lett. 73 (1998) 288.
[26]R.F. Haglund Jr., L. Yang, R.H. Magruder III, C.W. White, R.A. Zuhr, L. Yang, R. Dorsinville, and R.R. Alfano, Nucl. Instr. Meth. B 91 (1994) 493.
[27]R.H. Magruder III, R.A. Zuhr, and D.H. Osborne Jr., Nucl. Instr. Meth. B 99 (1995) 590.
[28]R.H. Magruder III, T.S. Anderson, R.A. Zuhr, and D.K. Thomas, Nucl. Instr. Meth. B 108 (1996) 305.
[29]R.A. Zuhr, R.H. Magruder, and T.S. Anderson, Surf. Coat. Technol. 103-104 (1998) 401.
[30]T.S. Anderson, R.H. Magruder III, R.A. Zuhr, and J.E. Wittig, J. Electr. Mater. 25 (1996) 27.
[31]E. Cattaruzza, G. Battaglin, R. Polloni, T. Cesca, F. Gonella, G. Mattei, C. Maurizio, P. Mazzoldi, F. D'Acapito, F. Zontone, and R. Bertoncello, Nucl. Instr. Meth. B 148 (1999) 1007.
[32]T.S. Anderson, R.H. Magruder III, J.E. Wittig, D.L. Kinser, and R.A. Zuhr, Nucl. Instr. Meth. (in press).
[33]M. Strobel, K.-H. Heinig, W. Moller, A. Meldrum, C.W. White, R.A. Zuhr, Nucl. Instr. Meth. B14 (1999) 343.
[34]S. Vijayalakshmi, H. Grebel, Z. Iqbal, and C.W. White, J. Appl. Phys. 84 (1998) 6502.
[35]A. Dowd, M. Samoc, B. Luther-Davies, and R.G. Elliman, Nucl. Instr. Meth. B 148 (1999) 964.
[36]S.V. Gaponenko, Optical Properties of Semiconductor Nanocrystals (Cambridge University Press, Cambridge UK 1998).
[37]K.S. Zhuralev, A.M. Gilinsky, and A.Y. Kobitsky, Appl. Phys. Lett. 73 (1998) 2962.
[38]T. Shimizu-Iwayama, D.E. Hole, and I.W. Boyd, J. Phys. Condens. Matter 11 (1999) 6595.
[39]E. Neufeld, S. Wang, R. Apetz, Ch. Buchal, R. Carius, C.W. White, and D.K. Thomas, Thin Sol. Films 294 (1997) 238.
[40]P. Mutti, G. Ghislotti, S. Bertoni, L. Bonoldi, G.F. Cerofolini, L. Meda, E. Grilli, and M. Guzzi, Appl. Phys. Lett. 66 (1995) 851.
[41]M.L. Brongersma, P.G. Kik, A. Polman, K.S. Min, and H.A. Atwater, Appl. Phys. Lett. 76 (2000) 351.
[42]M.L. Brongersma, A. Polman, K.S. Min, and H.A. Atwater, J. Appl. Phys. 86 (1999) 759.
[43]C.W. White, S.P. Withrow, A. Meldrum, J.D. Budai, D.M. Hembree, J.G. Zhu, D.O. Henderson, and S. Prawer, Mat. Res. Soc. Symp. Proc. 507 (1998) 249.
[44]N.F. Mott and E.A. Davies, Electronic Properties in Non-Crystalline Materials (Clarendon Press, Oxford, 1979).
[45]D.O. Henderson, M. Wu, R. Mu, A. Ueda, C.W. White, A. Meldrum, and A. Hepp, Invited Oral presentatation, Mater. Res. Soc. Fall Meeting (1998).
[46]K.S. Min, K.V. Scheglov, C.M. Yang, H.A. Atwater, M.L. Brongersma, and A. Polman, Appl. Phys. Lett. 69 (1996) 2033.
[47]S.P.Withrow, C.W. White, A. Meldrum, J.D. Budai, D.M. Hembree Jr., and J.C. Barbour, J. Appl. Phys. 86 (1999) 396.
[48]A. Meldrum, C.W. White, L.A. Boatner, R.A. Zuhr, I.M. Anderson, E. Sonder, and D.O. Henderson, Nucl. Instr. Meth. B 148 (1999) 957.
[49]J.D. Budai, C.W. White, S.P. Withrow, M.F. Chisholm, J.G. Zhu, and R.A. Zuhr, Nature 390 (1997) 384.
[50]A. Meldrum, E. Sonder, R.A. Zuhr, I.M. Anderson, J.D. Budai, C.W. White, L.A. Boatner, and D.O. Henderson, J. Mater. Res. 14 (1999) 4489.
[51]C.W. White, J.D. Budai, S.P. Withrow, J.G. Zhu, E. Sonder, R.A. Zuhr, A. Meldrum, D.M. Hembree, D.O. Henderson, and S. Prawer, Nucl. Instr. Meth. B 141 (1998) 228.
[52]C.W. White, J.D. Budai, J.G. Zhu, S.P. Withrow, D.M. Hembree, D.O. Henderson, A. Ueda, Y.S. Tung, and R. Mu, Mat. Res. Soc. Symp. Proc. 396 (1996) 397.
[53]C. Bonafos, B. Garrido, M. López, A. Romano-Rodríguez, O. Gonzáles-Varona, A. Pérez-Rodríguez, and J.R. Morante, Appl. Phys. Lett. 72 (1998) 3488.

[54]L.E. Brus, J. Chem. Phys. 80 (1984) 4403.
[55]C. Bonafos, B. Garrido, M. López, A. Romano-Rodríguez, O. González-Varona, A. Pérez-Rodríguez, J.R. Morante, and R. Rodríguez, Nucl. Instr. Meth. B 147 (1999) 373.
[56]M. Strobel, K.-H. Heinig, and W. Möller, Nucl. Instr. Meth. B 148 (1999) 104.
[57]A. Meldrum, L.A. Boatner, C.W. White, and R.C. Ewing, Mater. Res. Innov. 3 (2000) 190.
[58]L.A. Gea, L.A. Boatner, J. Rankin, and J.D. Budai (1995) Mat. Res. Soc. Symp. Proc. 354 (1995) 269.
[59]L.A. Gea, J.D. Budai, and L.A. Boatner, J. Mater. Res. 14 (1999) 2602.
[60]D.N. Lambeth, E.M.T. Velu, G.H. Bellesis, L.L. Lee, and D.E. Laughlin, J. Appl. Phys. 79 (1996) 4496.
[61]J.P. Jacubovics, Magnetism and Magnetic Materials. Institute of Metals, London, UK, 1987.
[62]E. Cattaruzza, F. Gonella, G. Mattei, P. Mazzoldi, D. Gatteschi, S. Sangregorio, M. Falconieri, G. Salvetti, and G. Battaglin, Appl. Phys. Lett. 73 (1998) 1176.
[63]T. Kobayashi, A. Nakanishi, F. Fukumura, and G. Langouche, J. Appl. Phys. 83 (1998) 4631.
[64]L. Gea, S. Honda, L.A. Boatner, T.E. Haynes, B.C. Sales, F.A. Modine, A. Meldrum, J.D. Budai, and L. Beckers, Mater. Res. Soc. Symp. Proc. 501, (1998) 137.
[65]S. Honda, F.A. Modine, A. Meldrum, J.D. Budai, T.E. Haynes, L.A. Boatner, and L.A. Gea, Mat. Res. Soc. Symp. Proc. 540 (1999) 225.
[66]S. Honda, F.A. Modine, T.E. Haynes, A. Meldrum, J.D. Budai, K.J. Song, J.R. Thompson, and L.A. Boatner, Mat. Res. Soc. Symp. Proc. 581 (in press).